

Local-moment magnetism in superconducting FeTe_{0.35}Se_{0.65} as seen via inelastic neutron scatteringZhijun Xu,^{1,2} Jinsheng Wen,^{1,3} Guangyong Xu,¹ Songxue Chi,⁴ Wei Ku,¹ Genda Gu,¹ and J. M. Tranquada¹¹*Condensed Matter Physics and Materials Science Department, Brookhaven National Laboratory, Upton, New York 11973, USA*²*Department of Physics, City College of New York, New York, New York 10033, USA*³*Department of Materials Science and Engineering, Stony Brook University, Stony Brook, New York 11794, USA*⁴*NIST Center for Neutron Research, National Institute of Standards and Technology, Gaithersburg, Maryland 20899, USA*

(Received 23 February 2011; published 11 August 2011)

The nature of the magnetic correlations in Fe-based superconductors remains a matter of controversy. To address this issue, we use inelastic neutron scattering to characterize the strength and temperature dependence of low-energy spin fluctuations in FeTe_{0.35}Se_{0.65} ($T_c \sim 14$ K). Integrating magnetic spectral weight for energies up to 12 meV, we find a substantial moment ($\langle M^2 \rangle_{LE} \sim 0.07\mu_B^2/\text{Fe}$) that shows little change with temperature, from below T_c to 300 K. Such behavior cannot be explained by the response of conduction electrons alone; states much farther from the Fermi energy must have an instantaneous local spin polarization. It raises interesting questions regarding the formation of the spin gap and resonance peak in the superconducting state.

DOI: 10.1103/PhysRevB.84.052506

PACS number(s): 74.70.Xa, 61.05.fg, 75.25.-j, 75.30.Fv

Antiferromagnetism and superconductivity are common to the phase diagrams of cuprate and Fe-based superconductors, and it is frequently proposed that magnetic correlations are important to the mechanism of electron pairing.^{1,2} Experiments on various Fe-based superconductors have demonstrated that magnetic excitations coexist with, and are modified by, the superconductivity. In particular, the low-energy spin excitation spectrum is modified by the emergence of a “resonance” peak and spin gap in the superconducting phase.^{3–11} The magnetic structures and excitations have been extensively studied by neutron scattering in these systems, including the AFe₂As₂ (“122”, A = Ba, Sr, Ca) system,^{3–6,12,13} the RFeAsO (“1111”, R = La, Ce, Pr, Nd, Gd, Sm) system,^{14–19} and the FeTe_{1–x}Se_x (“11”) system.^{7–11,20,21} Despite some variation in the magnetic structure of the parent compounds, in all known Fe-based superconductors, the “resonance” occurs at the same $\mathbf{Q}_0 \sim (0.5, 0.5, 0)$ (in the 2-Fe unit cell unit). At low temperature, the resonance is also accompanied by a well-defined but anisotropic dispersion^{10,11,20} along the transverse direction, with a spin gap below which there is no spectral weight in the superconducting state, resembling the spin excitations in many high T_c cuprates.^{22–25}

One essential and currently unsettled issue is the nature of the magnetism in the Fe-based superconductors.² In contrast to the Mott-insulating parent compounds of the cuprates, the parent compounds of all of the Fe-based superconductors are poor metals. This naturally leads to the suggestion of itinerant magnetism resulting from the nesting of the Fermi surface, or more generally, enhancement of noninteracting susceptibility.²⁶ Disregarding the apparent failure of such an itinerant picture in producing the so-called bi-collinear magnetic structure of Fe_{1+y}Te,²⁷ the spin-fluctuation picture of superconductivity²⁶ is qualitatively appealing, and appears to give a natural explanation for the spin resonance and spin gap.²⁸ Nevertheless, there are recent theoretical analyses that suggest that there may be a significant local-moment character to the magnetism, as a consequence of Hund’s rule coupling among Fe 3*d* electrons.²⁹ A direct way to test the different theoretical perspectives is to evaluate the instantaneous moment from inelastic magnetic neutron scattering measurements. This is the goal of the present work.

In this paper, we report an inelastic neutron scattering study on the temperature evolution of the low-energy magnetic excitation of an FeTe_{1–x}Se_x sample with $x = 65\%$. The magnetic excitations below $T_c \sim 14$ K are almost identical to those measured previously on superconducting FeTe_{1–x}Se_x samples with $x = 50\%$,^{7–11,20} having a spin gap of ~ 5 meV and a resonance at ~ 7 meV, with anisotropic dispersion along the direction transverse to \mathbf{Q}_0 . On heating to $T = 25$ K, the resonance disappears, with spectral weight moving into the gap. The \mathbf{Q} dependence of the spectrum is still narrow around $\hbar\omega \sim 5$ –6 meV, but appears to disperse outward for energies both above and below, similar to the those observed in the cuprates.^{22–24,30} With further heating, the spin excitations near the saddle point (~ 5 meV) start to split in \mathbf{Q} and become clearly incommensurate, exhibiting a “waterfall” structure at 100 K and above, similar to the situation in underdoped YBa₂Cu₃O_{6+x}.²⁴ However, the integrated spectral weight below $\hbar\omega = 12$ meV remains almost unchanged as a function of temperature, indicating a large energy scale associated with the stability of the instantaneous magnetic moment. The absolute normalization of the low-energy (LE) weight gives a lower limit (not counting the strong spectral weight at higher energies⁸) of $\langle M^2 \rangle_{LE} \sim 0.07\mu_B^2/\text{Fe}$. Such a robust and sizable moment is apparently beyond the standard consideration of the spin-density-wave picture²⁶ and strongly suggests that local-moment magnetism is present in the Fe-based superconductors.²⁹

The single-crystal sample used in the experiment was grown by a unidirectional solidification method with nominal composition of Fe_{0.98}Te_{0.35}Se_{0.65} (8.6 g). The bulk susceptibility, measured with a superconducting quantum interference device (SQUID) magnetometer, is shown in Fig. 1(b), indicating $T_c \sim 14$ K. Neutron scattering experiments were carried out on the triple-axis spectrometer BT-7 located at the NIST Center for Neutron Research. We used beam collimations of open-50’-S-50’-open (S = sample) with fixed final energy of 14.7 meV and two pyrolytic graphite filters after the sample. The lattice constants for the sample are $a = b = 3.81$ Å, and $c = 6.02$ Å, using a unit cell containing two Fe atoms. The inelastic scattering measurements have been performed in the ($HK0$) scattering plane [Fig. 1(a)]. The data are

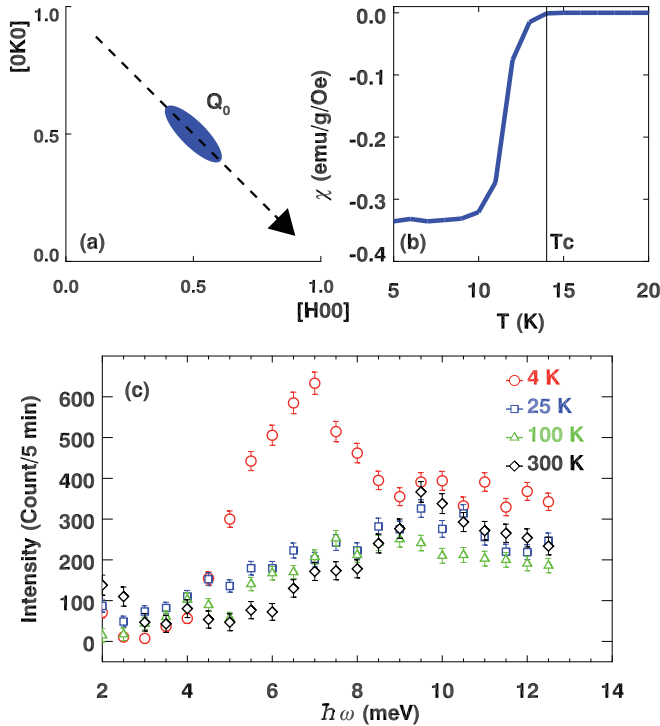


FIG. 1. (Color online) (a) The schematic diagram of the neutron scattering measurements in the $(HK0)$ zone. Dashed lines denote linear scans performed across $\mathbf{Q}_0 = (0.5, 0.5, 0)$ in the text. (b) ZFC magnetization measurements by SQUID with a 5 Oe field perpendicular to the a - b plane. $T_c \sim 14$ K is marked by a dashed line. (c) Constant Q scans at \mathbf{Q}_0 taken at different temperatures: 5 K (red circles), 25 K (blue squares), 100 K (green triangles), and 300 K (black diamonds). Fitted background obtained from constant energy scans has been subtracted from all data sets.

described in reciprocal lattice units (r.l.u.) of $(a^*, b^*, c^*) = (2\pi/a, 2\pi/b, 2\pi/c)$. Absolute normalizations are performed based on measurements of incoherent elastic scattering from the sample.

Low-energy spin excitations are mainly distributed near the \mathbf{Q}_0 in-plane wave vector, similar to the case in the 50% Se doped sample.³² In Fig. 1(c), we show constant- Q scans at \mathbf{Q}_0 from 4 to 300 K. There is a clear resonance peak for data taken in the superconducting phase ($T = 4$ K, red circles). When heated above T_c , the resonance peak disappears, and spectral weight starts to fill in the gap below $\Delta \sim 5$ meV. For the normal state, the intensity at \mathbf{Q}_0 appears to peak at around $\hbar\omega \sim 10$ meV. These results are in good agreement with previous neutron scattering measurements,^{7,10} indicating that further Se doping above the optimal value of 50% does not significantly alter the low-energy magnetic excitations in the system.

Constant energy scans across \mathbf{Q}_0 , performed in the transverse direction, are plotted in Fig. 2. One can see how the resonance disappears with heating in Figs. 2(c) and 2(d). For $\hbar\omega \leq 6.5$ meV, Figs. 2(a)–2(c), we note that the peak on the right side [larger K side, near $(0.25, 0.75, 0)$] is further out in Q , with respect to Q_0 , compared to its counterpart on the left (small K) side, and becomes disproportionately strong. This behavior is inconsistent with crystal symmetry,

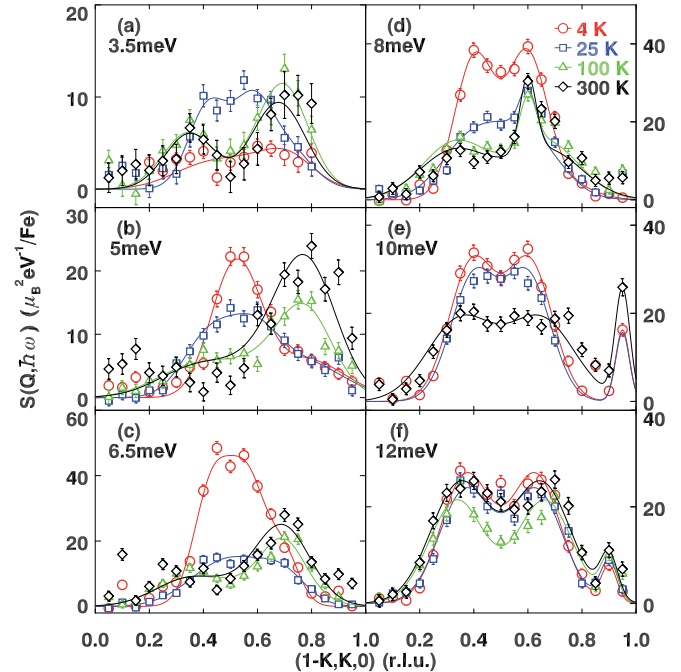


FIG. 2. (Color online) Constant energy scans at $(1 - K, K, 0)$ with different temperatures: 4 K (red circles), 25 K (blue squares), 100 K (green triangles), and 300 K (black diamonds) at different $\hbar\omega$: (a) 3.5 meV, (b) 5 meV, (c) 6.5 meV, (d) 8 meV, (e) 10 meV, and (f) 12 meV. A flat fitted background has been subtracted from all data sets. The solid lines are based on the fit described in the text. The error bars represent the square root of the number of counts.

which magnetic or simple phonon scattering must follow. The nature of this spurious peak is not entirely known. It is very likely not associated with magnetic scattering from the sample; its growth with temperature suggests that it arises from multiscattering processes involving certain phonon modes. Fortunately, it only appears on the large K side, leaving the small K side uncontaminated. In our data analysis, we fit the magnetic signal using a double Gaussian function, with two peaks split symmetrically about \mathbf{Q}_0 , plus a single Gaussian function for the spurious peak. The fitted magnetic intensities are presented as contour maps in Fig. 3. With the spurious peak removed, one can easily see the evolution of the magnetic excitation spectrum with temperature.

In the superconducting phase, Fig. 3(a), there is very little spectral weight below 5 meV, while the excitations disperse outward at higher energies. As a function of temperature [Figs. 3(a)–3(d)], the dispersion at the highest energies changes little, and one can still observe well-defined magnetic excitations at $\hbar\omega = 12$ meV up to $T = 300$ K. The temperature effect on the dispersion below the resonance energy is much more pronounced. On warming from 4 to 25 K, intensity that emerges below the gap appears to disperse outward slightly, as shown in Fig. 3(b). Our results are consistent with those in Ref. 11, where the spectrum is narrowest in Q at the saddle point around 5 meV, and becomes broader for energy transfers both above and below for $T > T_c$.

With further heating, the Q dependence of the spectrum changes most dramatically near the saddle point. At $T = 100$ K, the lower part of the dispersion clearly moves

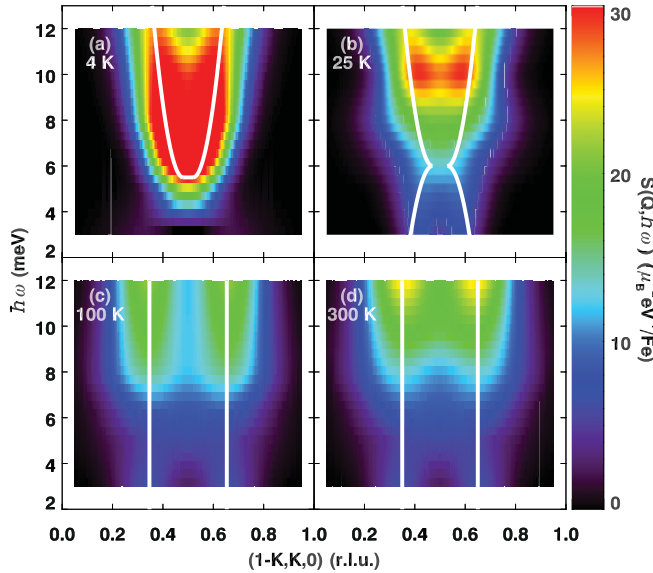


FIG. 3. (Color online) Contour intensity maps showing the fitted magnetic scattering intensity versus $\hbar\omega$ and \mathbf{Q} at different temperatures: (a) 4 K, (b) 25 K, (c) 100 K, and (d) 300 K.

outward from \mathbf{Q}_0 , as shown in Fig. 3(c). The saddle point at 5 meV actually disappears, and the dispersion becomes clearly incommensurate and almost vertical. There is little change between 100 and 300 K.

In Figs. 4(a) and 4(b), we plot the intensities, integrated along $\mathbf{Q} = (1 - K, K, 0)$, of the magnetic scattering and the spurious peak. The effect of the resonance in the superconducting phase is observable up to $\hbar\omega \sim 10$ meV. The plot of the spurious-peak intensity shows signs of temperature activation, and is peaked near 5 meV; in any case, its scale is generally small compared to the magnetic signal.

The magnetic response in the normal state shows little temperature dependence and the main spectral weight is

always located at higher energies (6 meV). Compared to that in the superconducting state, the low-energy spectral weight (below the gap) does appear to increase in the normal state when the “resonance” near 6.5 meV disappears, but remains almost unchanged with further heating for T up to 300 K. This is consistent with the system having no static magnetic order at low temperature, and therefore no shift of spectral weight from the elastic channel into those at low-energy transfers upon heating. The lack of temperature dependence for the magnetic excitation spectrum in the normal state for T between 25 and 300 K, suggests a large energy scale associated with the magnetic response. We also note that the dispersion changes from a near hour-glass shape at low temperatures ($T = 4$ K and 25 K) to a “waterfall” shape at high temperatures ($T = 100$ K and 300 K). This change in dispersion is qualitatively similar to the behavior reported for underdoped $\text{YBa}_2\text{Cu}_3\text{O}_{6+x}$,²⁴ but occurs at temperatures well within the normal state, and its origin is not entirely understood.

Our key result is obtained by integrating the magnetic signal over \mathbf{Q} and $\hbar\omega$. The measured inelastic magnetic scattering intensity is proportional to the dynamic spin correlation function $S(\mathbf{Q}, \omega) = \chi''(\mathbf{Q}, \omega)/(1 - e^{-\hbar\omega/k_B T})$, which follows the “sum rule” that $\int_{\text{BZ}} d\mathbf{Q} \int_{-\infty}^{+\infty} S^{\alpha\beta}(\mathbf{Q}, \omega) d\omega = \frac{1}{3v^*} \delta_{\alpha\beta} \langle M^2 \rangle / g^2$, where v^* is the volume of the Brillouin zone. By integrating the normalized spectral weight up to $\hbar\omega \sim 12$ meV, we can obtain a lower bound of the magnetic moment per Fe. For the \mathbf{Q} integration, we assume the peak width along the longitudinal direction is the same as transverse direction and that the response is uniform along L , based on results from previous measurements.^{7,10} For energy, we integrated over the interval $0 \text{ meV} \leq \hbar\omega \leq 12 \text{ meV}$, using the low-energy extrapolation indicated by the dashed lines in Fig. 4(a). From this integral, we obtain a spectral weight of $\langle M^2 \rangle_{\text{LE}} = 0.07(3) \mu_B^2$ per Fe. The temperature dependence of this quantity is negligible, as shown in Fig. 4(c). Similar behavior showing little temperature dependence of the integrated spectral weight is also evidenced in the AFM insulator La_2CuO_4 ³³ where magnetism is dominated by local moments.

The moment we have evaluated is only a small fraction of the total moment per site, considering that previous measurements have shown significant spectral weight all the way up to a few hundred meV.⁸ Nevertheless, such a large low-energy magnetic response is already an order of magnitude larger than what is expected from a simple itinerant picture. For example, taking the density of states³⁴ at the Fermi energy of ~ 1.5 states/eV from a nonmagnetic LDA calculation for FeSe, the corresponding bare susceptibility, or $\langle M^2 \rangle_{\text{LE}}$ derived from electrons near the Fermi level can be estimated to be no more than of order $0.001 \mu_B^2$ per Fe within an excitation energy range of 12 meV. Even including a mass enhancement factor of 2 to 3 as observed by photoemission,^{35,36} the resulting spectral weight is still at least an order of magnitude smaller than our observation. One could in principle fine-tune the interaction strength to bring the magnon pole to a very low energy to enhance the spectral weight, but then it will surely generate a strong temperature dependence of the spectral weight,³⁷ in drastic contrast to our observation. The observed lack of temperature dependence suggests that electronic states over a large energy range contribute to the effective moment, which is

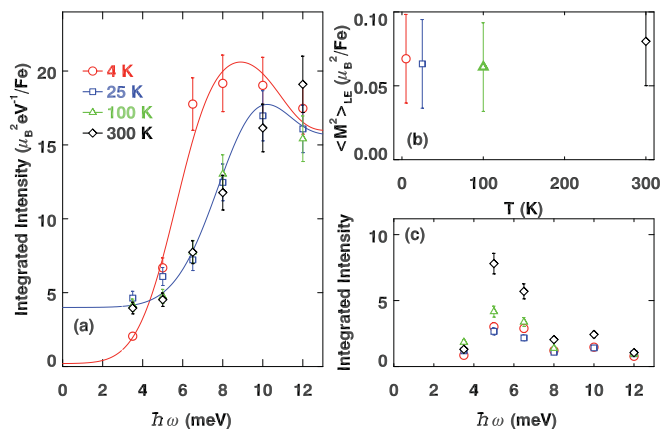


FIG. 4. (Color online) (a) \mathbf{Q} -integrated (integrated only in one dimension, along the transverse direction) magnetic intensity, obtained based on the fit described in the text, plotted vs temperature. (b) Average squared magnetic moment per Fe site vs temperature, for spectral weight integrated over $0 < \hbar\omega < 12$ meV. (c) \mathbf{Q} -integrated intensity for the spurious peak around $(0.25, 0.75, 0)$, plotted vs temperature.

consistent with having a significant local moment, as suggested by recent theoretical work.²⁹

We are, of course, not suggesting that the system should behave like an insulator with only a local-moment contribution to the magnetism. Apparently the rodlike dispersion we observe cannot be explained by spin-wave excitations emerging from a Heisenberg Hamiltonian. Nevertheless, our results do suggest that the simplest itinerant picture of weakly interacting electrons cannot be used to quantitatively explain the large, temperature-independent magnet moment in neutron scattering measurements. In addition to states near the Fermi surface, states at higher energies will have to be considered (nonperturbatively) when magnetism as well as superconductivity are concerned.

This leads to an interesting question. For the itinerant picture, the spin gap and resonance come out naturally from the pairing gap for the quasiparticles—although they are sensitive to the symmetry of the order parameter. If the

magnetic moments involve states at high binding energies, then one must reconsider the evaluation of the resonance. It is clear that the magnetic correlations are sensitive to the development of pairing and superconductivity; however, the electrons involved in the pairing and in the magnetism are not necessarily identical. Similar issues have been raised in the case of cuprates. These issues also raise questions concerning the nature of the pairing mechanism.

ACKNOWLEDGMENTS

We thank Weiguo Yin and Igor Zaliznyak for useful discussions. This work is supported by the Office of Basic Energy Sciences, US Department of Energy under Contract No. DE-AC02-98CH10886. J.S.W. and Z.J.X. are supported by the same source through the Center for Emergent Superconductivity, an Energy Frontier Research Center.

-
- ¹I. I. Mazin, *Nature (London)* **464**, 183 (2010).
²J. Paglione and R. L. Greene, *Nat. Phys.* **6**, 645 (2010).
³A. D. Christianson *et al.*, *Nature (London)* **456**, 930 (2008).
⁴M. D. Lumsden *et al.*, *Phys. Rev. Lett.* **102**, 107005 (2009).
⁵S. Chi *et al.*, *Phys. Rev. Lett.* **102**, 107006 (2009).
⁶D. S. Inosov *et al.*, *Nat. Phys.* **6**, 178 (2010).
⁷Y. Qiu *et al.*, *Phys. Rev. Lett.* **103**, 067008 (2009).
⁸M. D. Lumsden *et al.*, *Nat. Phys.* **6**, 182 (2010).
⁹J. Wen, G. Xu, Z. Xu, Z. W. Lin, Q. Li, Y. Chen, S. Chi, G. Gu, and J. M. Tranquada, *Phys. Rev. B* **81**, 100513(R) (2010).
¹⁰S. H. Lee *et al.*, *Phys. Rev. B* **81**, 220502 (2010).
¹¹S. Li *et al.*, *Phys. Rev. Lett.* **105**, 157002 (2010).
¹²J. Zhao *et al.*, *Nat. Phys.* **5**, 555 (2009).
¹³H. Chen *et al.*, *EuroPhys. Lett.* **85**, 17006 (2009).
¹⁴C. de la Cruz *et al.*, *Nature (London)* **453**, 899 (2008).
¹⁵J. Zhao *et al.*, *Nat. Mater.* **7**, 953 (2008).
¹⁶Q. Huang, J. Zhao, J. W. Lynn, G. F. Chen, J. L. Luo, N. L. Wang, and P. Dai, *Phys. Rev. B* **78**, 054529 (2008).
¹⁷C.-H. Lee *et al.*, *J. Phys. Soc. Jpn.* **77**, 083704 (2008).
¹⁸J. Zhao *et al.*, *Phys. Rev. B* **78**, 132504 (2008).
¹⁹Y. Qiu *et al.*, *Phys. Rev. B* **78**, 052508 (2008).
²⁰D. N. Argyriou *et al.*, *Phys. Rev. B* **81**, 220503 (2010).
²¹T. J. Liu *et al.*, *Nat. Mater.* **9**, 718 (2010).
²²S. M. Hayden *et al.*, *Nature (London)* **429**, 531 (2004).
²³B. Vignolle *et al.*, *Nat. Phys.* **3**, 163 (2007).
²⁴V. Hinkov *et al.*, *Nat. Phys.* **3**, 780 (2007).
²⁵G. Xu *et al.*, *Nat. Phys.* **5**, 642 (2009).
²⁶I. I. Mazin, D. J. Singh, M. D. Johannes, and M. H. Du, *Phys. Rev. Lett.* **101**, 057003 (2008); K. Kuroki, S. Onari, R. Arita, H. Usui, Y. Tanaka, H. Kontani, and H. Aoki, *ibid.* **101**, 087004 (2008); M. Daghofer, A. J. Riera, E. Arrigoni, J. D. Scalapino, E. Dagotto *ibid.*, **101**, 237004 (2008); J. Knolle, I. Eremin, A. V. Chubukov, and R. Moessner, *Phys. Rev. B* **81**, 140506 (2010).
²⁷W. Bao *et al.*, *Phys. Rev. Lett.* **102**, 247001 (2009); S. Li *et al.*, *Phys. Rev. B* **79**, 054503 (2009).
²⁸T. A. Maier, S. Graser, D. J. Scalapino, and P. Hirschfeld, *Phys. Rev. B* **79**, 134520 (2009).
²⁹I. I. Mazin and M. D. Johannes, *Nat. Phys.* **5**, 141 (2009); S.-P. Kou, T. Li, and Z.-Y. Weng, *EuroPhys. Lett.* **88**, 17010 (2009); L. de'Medici, S. R. Hassan, and M. Capone, *J. Supercond. Nov. Magn.* **22**, 535 (2009); W.-G. Yin, C.-C. Lee, and W. Ku, *Phys. Rev. Lett.* **105**, 107004 (2010); R. Arita and H. Ikeda, *J. Phys. Soc. Jpn.* **78**, 113707 (2009); K. Haule and G. Kotliar, *New J. Phys.* **11**, 025021 (2009).
³⁰G. Xu, J. M. Tranquada, T. G. Perring, G. D. Gu, M. Fujita, and K. Yamada, *Phys. Rev. B* **76**, 014508 (2007).
³¹There is no elastic magnetic intensity found near (0.5,0,0.5), which is the antiferromagnetic ordering wave vector in the parent compound, and very little spectral weight near (0.5,0,0) at low energies and low temperature.
³²Z. Xu, J. Wen, G. Xu, Q. Jie, Z. Lin, Q. Li, S. Chi, D. K. Singh, and G. Gu, and J. M. Tranquada, *Phys. Rev. B* **82**, 104525 (2010).
³³K. Yamada, K. Kakurai, Y. Endoh, T. R. Thurston, M. A. Kastner, R. J. Birgeneau, G. Shirane, Y. Hidaka, and T. Murakami, *Phys. Rev. B* **40**, 4557 (1989).
³⁴K. W. Lee, V. Pardo, and W. E. Pickett, *Phys. Rev. B* **78**, 174502 (2008).
³⁵A. Tamai *et al.*, *Phys. Rev. Lett.* **104**, 097002 (2010).
³⁶Y. Zhang *et al.*, *Phys. Rev. B* **82**, 165113 (2010).
³⁷T. Kariyado and M. Ogata, *J. Phys. Soc. Jpn.* **78**, 043708 (2009).